ISSN (Online) : 2319 - 8753
ISSN (Print) : 2347 - 6710

International Journal of Innovative Research in Science, Engineering and Technology

Volume 3, Special Issue 3, March 2014

2014 International Conference on Innovations in Engineering and Technology (ICIET'14)
On 21st & 22nd March Organized by

K.L.N. College of Engineering, Madurai, Tamil Nadu, India

A Novel Approach for Retinal Lesion Detection Diabetic Retinopathy Images

M. Sridevi Maheswari [#1], Adarsh Punnolil[*2]

Dept. of ECE, Dr. Nallini Institute of Engineering and Technology, Dharapuram, Tamilnadu, India

Dept. of ECE, Dr. Nallini Institute of Engineering and Technology, Dharapuram, Tamilnadu, India

ABSTRACT— In the modern world, diabetic retinopathy (DR) has become one of the most severe complication prevalent among diabetic patients. The success rate of its curability solemnly depends on the early stage diagnosis or else will lead to total blindness. The paper proposes a novel method for the automated identification of exudates pathologies in retinopathy fundus images based on computational intelligence technique. Approach employs a unique sequential execution of morphological operators to extract fundus image features like vessels, red lesions, and white lesions together with texture feature analysis. Finally features selected are passed into the well-known support vector machine (SVM) classifier which classifies the images into normal and abnormal classes. Real time and publicly available database analysis shows really encouraging performance metrics of the proposed method in terms of sensitivity, specificity and accuracy.

KEYWORDS— Diabetic retinopathy, red lesions, white lesions, support vector machine.

I. INTRODUCTION

Robust screening methods increases the accessibility of eye care providers with timely intervention of to prevent the vision loss caused by diabetic retinopathy (DR) [1]. Digital color fundus photography has become a pre-requisite for automated DR detection due to its patient friendliness and cost effectiveness [2]. Recently a study by International Diabetes Federation found diabetes will see an epidemic growth closing to 552 million people by 2030 [3]. Besides this complications arising from diabetes are also growing including DR, which is the root cause of blindness within the 20–74 age group in most of the developed countries and presently affect 2–4% of diabetic people [4]-[6].

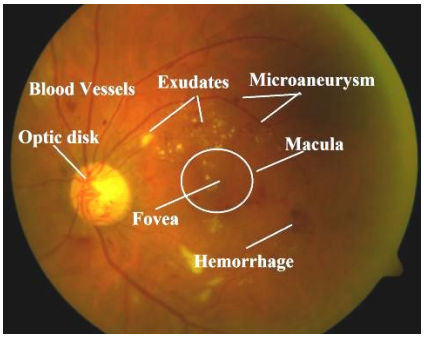

Fig. 1. Retinal main regions and DR related pathologies

The most common signs of DR are red lesions (microaneurysms, hemorrhages) and bright lesions (exudates, drusen and cotton wool spots). The presence of red lesions and/or hard exudates (bright lesions) are indicative of early stage DR. Microaneurysms (MAs) are focal dilatations of retinal capillaries and appear as red dots in retinal fundus images. Bright lesions or intra-retinal lipid exudates results from the breakdown of blood retinal barrier. Excluded fluid rich in lipids and proteins leave the parenchyma, leads to retinal edema and exudation. Lastly, wherever capillary walls are weak inside the retina, dot hemorrhages lesions are found which are slightly larger than MAs. On rupturing it will cause intra-retinal hemorrhages. Progression of DR also causes macular edema, neo-vascularization and in later stages, retinal detachment. All these abnormalities are depicted in Fig. 1 with main retinal structures highlighted.

Systematic screening by eye care specialists of diabetic patients is a cost-effective health care practice that can diagnose the pathology at the initial stage [7], [8]. In order to accommodate the screening and annual reviews requisite of a large number of patients, an automated screening tool is a useful adjunct in diabetes clinics. At present, there are several methods which can accurately diagnose specific DR related lesions [9]–[11].

All the existing methodologies require different pre and post-processing steps depending on the lesion of interest, color normalization and resolution corrections to account for images with different ethnicity and field of view [12].

II. State of Art

A lot of studies have investigated the automated detection of diabetic retinopathy by diagnosing red lesions [13]–[16], and bright lesions [17]–[21]. Methodology in [22] classified pixels using a neural network scheme and represented pixels using a computation based on 7-D vector composed of gray-level and moment invariants-based features. Vessel-like candidate segments detected using a method based on watershed lines and ridge strength measurement to train SVM, was applied by [23]. In [24] DR related lesions from fundus images was identified using visual word dictionary representing points of interest (PoIs), that contain regions associated with DR related pathology.

Approach of [25] applied a splat-based feature supervised classification method to detect large, uneven hemorrhage detection in fundus photographs. MA detection through the analysis of directional cross-section profiles centered on the local maximum pixels of the pre-processed image followed by a Naive Bayes classification using the statistical measures of the corresponding profiles was done in [26]. Another algorithm in [27] assessed the need for referral in DR detection with a decision based on the fusion of results by meta-classification. Reference [28] modelled a clutter labeling technique that attempts to address the discrimination of MAs and postpone the target modeling together with progressive rejection of clutter responses and target recognition if fewer clutter responses remain in the end.

In this paper a new approach has been proposed which can be effectively used for automated diagnosis of DR. The algorithm we developed is based on a sequential execution of morphological operators as well as machine learning technique. The approach find very effective in detecting major DR pathologies like red lesions, bright lesions and white lesions together with extracting the vasculature within the retina (Fig. 2). The rest of the work is organized as follows: Section III describes proposed lesion detection algorithm, Section IV discusses the experimental results and performance evaluation, and finally concluding remarks in Section V.

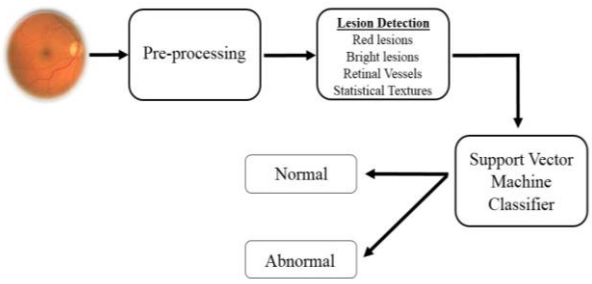

Fig. 2 Basic block diagram of lesion detection algorithm

III. Proposed Lesion Detection Method

A. Image Acquisition

The methodology described here, is evaluated on two publicly available databases: DRIVE [29] and STARE [30]. These databases have been widely used by other researchers to check the effectiveness of their segmentation methods.

The 40 color fundus retinal images of DRIVE database were captured with a Canon CR5 non-mydriatic 3CCD camera with a 45^0 field-of-view (FOV). Each image represented in 8 bits per color plane, captured at 768 x 584 pixels, and were saved in JPEG format. Hoovers' [38] STARE database comprises of 81 retinal color fundus images taken with a TopCon TRV-50 fundus camera at 35^0 FOV. The database is available in PPM format at 700 x 605 pixels, in 8 bits per color channel form. Details of database is in Table I.

TABLE I
Entire Data Set Categorisation

Source	Total Images	Normal	Abnormal
DRIVE	40	33	7
STARE	81	30	51
Total	121	63	58

B. Preprocessing

All the images were resized to 720 × 576 pixels while maintaining the original aspect ratio prior to analysis. Following this, green color plane was used in the analysis since it shows the best contrast between the background retina and the vessels. The grey levels were normalized by stretching the image contrast using CLAHE to cover the full pixel dynamic range, excluding the surrounding dark border pixels and any image labels. CLAHE limits amplifying any noise that might be present in the low contrast area of the image.

C. Retinal Vasculature Extraction

Initially, the green component's intensity is inverted. After inverting the green component's intensity, edge detection ζ is performed using canny method.

TABLE II
Vessel Segmentation Algorithm

Input :	Green channel retinal fundus image (I_g)
Output :	Blood vessels extracted image (I_{vsl})
Step 1	Inversion of (I_g) to $(-I_g)$
Step 2	Applied with canny edge operator ζ
Step 3	Border detection and initial vessel segmentation
Step 4	Morphological opening operation (α) with disk shaped structuring element
Step 5	Contrast enhancement followed by (α) with ball shaped structuring element
Step 6	Thresholding and median filtering
Step 7	Subtracting **3rd** and **6th** Steps followed by 'imfill' function gives final output (I_{vsl})

The border is then detected and a disk shaped structuring element (SE) of radius 8 is created with morphological opening operation (erosion followed by dilation). Next, subtract the eroded image with the original image and the border or boundary is obtained.

Afterwards, adaptive histogram equalization (CLAHE) is performed to improve the contrast of the image and to correct uneven illumination. A morphological opening operation (erosion then dilation) is performed to highlight the blood vessels. The image is then subtracted from the adaptive histogram equalized image. From the subtracted image, the image is converted from grayscale to binary by performing thresholding with value of 0.1. Median filtering is performed to remove "salt and pepper" noise. The boundary is obtained after subtracting the border with disk shaped SE from image with median filtering. The border is then eliminated after filling the holes that do not touch the edge to obtain the final image (Fig. 3). The pixel values of the image are inverted to get only the blood vessels with black background. Table II describes the blood vessel algorithm.

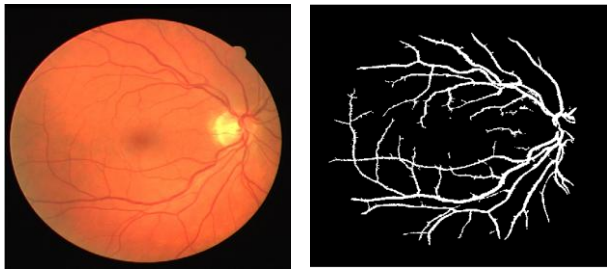

(a) (b)

Fig. 3 Retinal vasculature extraction illustrated using DRIVE database (a) input image (b) vessel extracted image.

D. Bright Lesions Segmentation

Exudates appear as bright yellow-white deposits on the retinal layer. Their shape and size varies gradually with different stages of retinopathy. Initially extracted green channel image is converted into grayscale image and then preprocessed for uniformity. Then morphological closing operation is carried out to remove the blood vessels.

TABLE III

EXUDATE SEGMENTATION ALGORITHM

Input :	Green channel retinal fundus image (I_g)
Output :	Exudate segmented image (I_{exd})
Step 1	Morphological closing operation (β) with octagon shaped structuring element (SE).
Step 2	Columnwise neighborhood operation (ψ)
Step 3	Thresholding followed by (β) with disk (SE)
Step 4	Applied with canny edge operator ζ
Step 5	Choosing a region of interest (ROI)
Step 6	Removal of optic disk and border.
Step 7	Morphological erosion operator (ρ) with disk (SE) to give final (I_{exd})

Morphological closing consists of dilation followed by erosion. The canny edge detector is used to detect the edges. Canny edge detector is an edge detecting operator that uses multistage algorithm to detect wide range of edges in images. Strong and weak fine blood vessels can be detected using this canny edge detector. In the beginning green channel image first finds the edges using canny method; before removing the circular border to fill the enclosed small area. Then circular border, edges and larger areas are removed. Being the bright spots on the image, adaptive histogram equalization is applied twice followed by image segmentation to make the exudates visible. Obtained bright features are then compared with large area removed image using AND logic in order to get rid of exudates (Fig. 4). Algorithm is detailed in Table III.

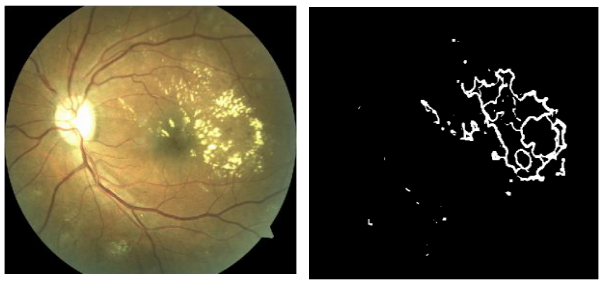

Fig. 4 Bright lesion detection illustrated using STARE database (a) input image (b) exudates detected image.

E. Red Lesions Detection

All MAs appear as tiny red dots on retinal fundus image. Therefore the red component of the RGB image are used to identify the MAs. Next, the intensity is then inverted. Similar to blood vessels detection, canny method is used for edge detection for MAs detection. The boundary is detected by filling up the holes and a disk shaped structuring element (SE) of radius 8 is created with morphological opening operation (erosion then dilation). The edge detected image is then subtracted from the image with boundary to obtain image without boundary.

After which, the holes or gaps are filled, resulting in MAs and other unwanted artifacts present. The image with filled holes or gaps then subtracts the image before filled holes or gaps. The resulting image thus has MAs and other unwanted artifacts without the edge.

TABLE IV

MICROANEURYSM SEGMENTATION ALGORITHM

Input :	Red channel retinal fundus image (I_r)
Output :	Microaneurysms segmented image (I_{ma})
Step 1	Inversion of (I_r) to $(-I_r)$
Step 2	Applied with canny edge operator ζ
Step 3	Border detection and operator (α) with disk shaped SE
Step 4	Boundary removal and hole filling with mutual subtraction between the outputs
Step 5	Vessel detection and ζ operation
Step 6	Subtract outputs of **4th** and **5th** steps
Step 7	Hole filling and subtraction from Step **6** to give final (I_{ma})

The blood vessels are detected using the same method. Edge detection canny method is then used on the blood vessels image to detect the edges. This image is then subtracted from the image after boundary subtraction. Finally, after filling the holes or gaps, this image is subtracted with the image with MAs and unwanted artifacts to obtain the final image with only MAs. Figure. 5 shows MAs detected images. Entire algorithmic process is explained in Table IV.

Fig. 5 Red lesions segmentation illustrated using STARE (a) input image (b) MAs segmented image.

F. Feature Extraction

Afterwards the pre-processing stage, the fundus images features viz: area of blood vessels, area of exudates, and area of microaneurysms are extracted along with texture properties. These metrics are later used to classify the images accurately.

1) Texture analysis: The function of spatial variation in pixel intensities (gray value) is known as image texture. The basic types of texture analysis computation are structural, statistical and spectral. The texture features considered for this work are mean, standard deviation (SD), third moment, entropy and homogeneity. Co-occurrence matrix captures the spatial distribution of gray level from which homogeneity can be obtained [31].

Let z_i denote the values of all possible intensities in an M x N image, where i=0,1,….,L-1. The probability, $p(z_k)$, of intensity level z_k occurring in a input image is specified by

$$p(z_k)= \frac{n_k}{MN} \quad (1)$$

where n_k is the number of times that intensity z_k occurs in the image and MN is the total number of pixels. Once we have $p(z_k)$, the mean intensity is given by

$$m= \sum_{k=0}^{L-1} n_k\, p(z_k) \quad (2)$$

Similarly standard deviation (SD) is a measure of the spread of the values of z about mean, and is given by square root of variance of the intensities,

$$\sigma= \sqrt{\sum_{k=0}^{L-1} (z_k - m)^2\, p(z_k)} \quad (3)$$

Third moment is a measure of the skewness of the histogram. It is given by:

$$\mu_3(z)= \sum_{k=0}^{L-1} (z_k - m)^3\, p(z_k) \quad (4)$$

Entropy is a statistical measure of the disorder or randomness in a grayscale image which is given by:

$$Entropy= -\sum p(z_k) \log_2 p(z_k) \quad (5)$$

GLCM is created by calculating how often a pixel with gray level value i occurs in a specific spatial relationship to a pixel with the value j. It returns a value between 0 and 1.

$$Homogeneity = \sum_{i,j} \frac{p(i,j)}{1+|i-j|} \quad (6)$$

There are now total of 7 features which include two area calculations (exudates and blood vessels) and five texture features.

G. Classification by SVM

In this paper, Support Vector Machine (SVM) is used to classify the images into normal and abnormal. The images with lesions are abnormal and images without lesions are normal.

The basic operation of binary SVM is by finding the hyper-plane that best separates vectors from both classes in feature space at the same time maximizing the distance from each class to the hyperplane. It includes both linear and nonlinear methods for this hyperplane creation [14]. If the two classes are linearly separable, SVM computes the optimal separating hyper-plane with the maximum margin by minimizing the objective function $\|w\|^2$ subject to:

$$(x_i \cdot w + b) y_i \geq 1, \quad (7)$$

Since SVM is a linear classifier, it has it limitation when a non-linear classification is needed. To overcome this Kernel functions can be used as a solution to nonlinear boundaries problems [32].

SVM is a concept in statistics and computer science for a set of related supervised learning methods that analyze data and recognize patterns, used for classification for each given input, which of two possible classes forms the output, making the SVM a non-probabilistic binary linear classifier. Given a set of training examples, each marked as belonging to one of two categories, an SVM training algorithm builds a model that assigns new examples into one category or the other. An SVM model is a representation of the examples as points in space, mapped so that the examples of the separate categories are divided by a clear gap that is as wide as possible. New examples are then mapped into that same space and predicted to belong to a category based on which side of the gap they fall on.

IV. EXPERIMENTAL RESULTS

To investigate the effectiveness of the proposed method, entire algorithm was run on all the datasets and results for exudates detection and Blood Vessels detection were collected. Time of MATLAB code for an image was 15 seconds, using a PC with an Intel i3 Processor and 2 GB RAM.

A. Performance Evaluation

All the data bases are individually used for training and testing the classifier. The samples of each dataset are divided into 90% training and 10% for testing. Then the SVM classifier is trained with the training data set. Later each of the test data set of the corresponding database is tested with SVM classifier. To evaluate the performance of the system; performance measures such as sensitivity, specificity and accuracy are calculated. The terms used to measure the test performance are true positive (TP), true negative (TN), false positive (FP), false negative (FN) and total number of images (N). Table V shows the results obtained for each test set of individual databases.

Table VI shows the performance comparison of the proposed method with the most related works in the literature [17], [33], [34]. It is worth notable that given approach was not only assesed on a larger dataset of retinal images (including 58 abnormal and 63 normal) but also generated performance metrics which is really competable with state-of-art in this area.

$$Sensitivity(\%) = \frac{TP}{TP + FN} \times 100\% \quad (8)$$

$$Specificity(\%) = \frac{TN}{TN + FP} \times 100\% \quad (9)$$

$$Accuracy(\%) = \frac{TP + TN}{N} \times 100\% \quad (10)$$

TABLE V
PERFORMANCE EVALUATION METRICS

Author	Sensitivity (%)	Specificity (%)	Accuracy (%)
DRIVE	88.9	91.2	93
STARE	86.4	91.7	93.5
Average	87.65	91.45	93.5

TABLE VI
PERFORMANCE COMPARISON WITH EXISTING SYSTEMS

Source	Images Used	Sensitivity (%)	Specificity (%)
Walter *et al.* [17]	30	100	88.6
Sinthanayothin *et al.* [33]	30	88.5	99.7
Chutatape *et al.* [34]	35	100	71
Proposed Method	121	87.65	91.45

V. DISCUSSION AND CONCLUSION

This paper explores methods for the purpose of detecting and classifying lesions. The out comings of all the performance analytics reveals that suggested technique really competes with the existing DR analysis methods. A possible reason for this is the novelty in the design of lesion detection algorithms that integrates well with SVM classifier. As SVM being a supervised classifier the drawback is the need for (manually) marked training information. But when working with autopsy relevant problems, performance is more important than time which is assured in our technique. Sturdiness and precision of the technique was calculated against ophthalmologist's hand-drawn ground-truth. All the results acquired are really motivating. As a scope for future work the method can be expanded using multiclass SVM's and including more number of feature set in order to decrease the chance of fatalness.

REFERENCES

[1] M. D. Abramoff, J. M. Reinhardt, S. R. Russell, J. C. Folk, V. B. Mahajan, M. Niemeijer, and G. Quellec, *"Automated early detection of diabetic retinopathy,"* *Ophthalmology*, no. 6, pp. 1147–1154, Apr.

[2] O. Faust, R. AcharyaU., E. Y. K. Ng,K.-H. Ng, and J. S. Suri, *"Algorithms for the automated detection* of diabetic retinopathy using digital fundus images: A review," *J. Med. Syst.*, Apr.

[3] World Health Organization. (2012, Sep.).*"Diabetes programme,"* [Online]. Available: http://www.who.int/diabetes/en

[4] N. Younis, D. M. Broadbent, S. P. Harding, and J. R. Vora, *"Prevalence of diabetic eye disease in patients entering a systematic primary care-based eye screening programme," Diabet. Med.*, vol. 19, pp. 1014–1021, 2002.

[5] H. Taylor, J. Xie, S. Fox, R. Dunn, A. Arnold, and J. Keeffe, *"The prevalence and causes of vision loss in indigenous australians: The national indigenous eye health survey," Med. J. Aust.*, vol. 192, no. 6, pp. 312–318, 2010.

[6] D. J. Pettitt, A. Okada Wollitzer, L. Jovanovic, G. He, and E. Ipp, *"Decreasing the risk of diabetic retinopathy in a study of case management: The california medical type 2 diabetes study," Diabetes Care*, vol. 28, pp. 2819–2822, 2005.

[7] Q. Mohamed, M. C. Gillies, and T. Y. Wong, "*Management of diabetic retinopathy: A systematic review," J. Amer. Med. Assoc.*, vol. 298, no. 8, pp. 902–916, 2007.

[8] M. James, D. A. Turner, D. M. Broadbent, J. Vora, and S. P. Harding, *"Cost effectiveness analysis of screening for sight threatening diabetic eye disease," Br. Med. J.*, vol. 320, pp. 1627–1631, 2000.

[9] L. Giancardo, F. Meriaudeau, T. Karnowski, Y. Li, K. Tobin, and E. Chaum, *"Microaneurysm detection with radon transform-based classification on retina images,"* in *Proc. Intl. Conf. IEEE Eng. Med. Biol. Soc.*, 2011, pp. 5939–5942.

[10] B. Antal, I. Lazar, A. Hajdu, Z. Torok, A. Csutak, and T. Peto, *"Evaluation of the grading performance of an ensemble-based microaneurysm detector,"* in *Proc. Intl. Conf. IEEE Eng. Med. Biol. Soc.*, 2011, pp. 5943–5946.

[11] A. D. Fleming, S. Philip, K. A. Goatman, J. A. Olson, and P. F. Sharp, "*Automated microaneurysm detection using local contrast normalization and local vessel detection," IEEE Trans. Med. Imag.*, vol. 25, no. 9, pp. 1223–1232, 2006.

[12] M. J. Cree, E. Gamble, and D. J. Cornforth, *"Colour normalization to reduce inter-patient and intra-patient variability in microaneurysm detection in colour retinal images,"* in *Proc. Workshop Digital Image Comput.*, 2005, pp. 163–168.

[13] J. H. Hipwell, F. Strachan, J. A. Olson, K. C. McHardy, P. F. Sharp, and J. V. Forrester, *"Automated detection of microaneurysms in digital red-free photographs: A diabetic retinopathy screening tool," Diabetic Med.*, vol. 17, pp. 588–594, 2000.

[14] M. Niemeijer, B. V. Ginneken, J. Staal, M. S. A. Suttorp-Schulten, and M. D. Abramoff, *"Automatic detection of red lesions in digital color fundus photographs," IEEE Trans. Med. Imag.*, vol. 24, no. 5, pp. 584–592, May 2005.

[15] A. D. Fleming, S. Philip, K. A. Goatman, J. A. Olson, and P. F. Sharp, *"Automated assessment of diabetic retinal image quality based on clarity and field definition," Investigative Ophthalmol. Vis. Sci.*, vol. 47, pp. 1120–1125, 2006.

[16] T. Walter, P. Massin, A. Erginay, R. Ordonez, C. Jeulin, and J. C. Klein, *"Automatic detection of microaneurysms in color fundus images," Med. Image Anal.*, vol. 11, pp. 555–566, 2007.

[17] T. Walter, J. C. Klein, P. Massin, and A. Erginay, *"A contribution of image processing to the diagnosis of diabetic retinopathy-detection of exudates in color fundus images of the human retina," IEEE Trans. Med. Imag.*, vol. 21, no. 10, pp. 1236–1243, Oct. 2002.

[18] A. Osareh, M. Mirmehdi, B. Thomas, and R. Markham, *"Automated identification of diabetic retinal exudates in digital colour images," Br. J. Ophthalmol.*, vol. 87, pp. 1220–1223, 2003.

[19] M. Niemeijer, B. V. Ginneken, S. R. Russel, M. S. A. Suttorp-Schulten, and M. D. Abramoff, *"Automated detection and differentiation of drusen, exudates and cotton-wool spots in digital color fundus photographs for diabetic retinopathy diagnosis," Investigate Ophthalmol. Vis. Sci.*, vol. 48, pp. 2260–2267, 2007.

[20] A. D. Fleming, S. Philip, K. A. Goatman, J. A. Olson, and P. F. Sharp, *"Automated detection of exudates for diabetic retinopathy screening," Phys. Med. Biol.*, vol. 52, pp. 7385–7396, 2007.

[21] C. I. Sánchez, M. García, A. Mayo, M. I. López, and R. Hornero, *"Retinal image analysis based on mixture models to detect hard exudates," Med. Image Anal.*, vol. 13, pp. 650–658, 2009.

[22] D. Marín, A. Aquino, M. E. G. Arias, and J. M. Bravo, *"A new supervised method for blood vessel segmentation in retinal images by using gray-level and moment invariants-based features," IEEE Trans. Med. Imag.*, vol. 30, no. 1, pp. 146–158, Jan. 2011.

[23] K. A. Goatman, A. D. Fleming, S. Philip, G. J. Williams, J. A. Olson, and P. F. Sharp, *"Detection of new vessels on the optic disc using retinal photographs," IEEE Trans. Med. Imag.*, vol. 30, no. 4, pp. 972–979, April. 2011.

[24] A. Rocha, T. Carvalho, H. F. Jelinek, S. Goldenstein, and J. Wainer, *"Points of interest and visual dictionaries for automatic retinal lesion detection," IEEE Trans. Biomed. Eng.*, vol. 59, no. 8, pp. 2244–2253, Aug. 2012.

[25] Li Tang, M. Niemeijer, J. M. Reinhardt, M. K. Garvin, and M. D. Abramoff, *"Splat feature classification with application to retinal hemorrhage detection in fundus images," IEEE Trans. Med. Imag.*, vol. 32, no. 2, pp. 364–375, Feb. 2013.

[26] I. Lazar, and A. Hajdu, *"Retinal microaneurysm detection through local rotating cross-section profile analysis," IEEE Trans. Med. Imag.*, vol. 32, no. 2, pp. 400–407, Feb. 2013.

[27] R. Pires, H. F. Jelinek, J. Wainer, S. Goldenstein, E. Valle, and A. Rocha, *"Assessing the need for referral in automatic diabetic retinopathy detection," IEEE Trans. Biomed. Eng.*, vol. 60, no. 12, pp. 3391–3398, Dec. 2012.

[28] K. Ram, G. D. Joshi, and J. Sivaswamy, *"A Successive Clutter-Rejection based Approach for Early Detection of Diabetic Retinopathy," IEEE Trans. Biomed. Eng.*, vol. 58, no. 3, pp. 664 - 673, March 2011.

[29] Research Section, Digital Retinal Image for Vessel Extraction (DRIVE) Database. Utrecht, The Netherlands, Univ. Med. Center Utrecht, Image Sci. Inst. [Online]. Available: http://www.isi.uu.nl/Re-search/Databases/DRIVE

[30] STARE Project Website. Clemson, SC, Clemson Univ. [Online]. Available: http://www.ces.clemson.edu/

[31] R. C. Gonzalez and R. E. Woods, *Digital Image Processing*, 2nd ed. Reading, MA: Addison-Wesley, 2002.

[32] V. Vapnik, *Statistical Learning Theory*, New York: Willey, 1998.